Polypropylene–Phenol Formaldehyde-Based Compatibilizers. III. Application in PP/PBT and PP/PPE Blends

K. LARSEN BØRVE,[1] H. K. KOTLAR,[2] C.-G. GUSTAFSON[1]

[1] The Norwegian Institute of Science and Technology, Department of Machine Design and Materials Technology, N-7034 Trondheim, Norway

[2] Statoil Research Centre, N-7005 Trondheim, Norway

Received 14 July 1997; accepted 1 October 1997

ABSTRACT: A new class of compatibilizers suitable for blends or alloys of polypropylene (PP) and engineering polymers having aromatic residues or functionality complimentary to hydroxyl were evaluated in blends of isotactic PP and poly(butylene terephthalate) (PBT), and poly(phenylene ether) (PPE) PP-based blends with 10–30 wt % PBT or PPE were studied. From response modeling of the PP/PBT and PP/PPE blends, it was evident that the viscosity ratio among the blend component, compatibilizer content, and PBT or PPE content were important for the final blend properties. Impact strength was observed to be the most sensitive response to blend compatibilization. The PP-*g*-PF compatibilizer was observed to be more efficient in blends of PBT than of PPE. The main reason for that was the availability of reactive end-groups in the case of PBT, making covalent bonding between the compatibilizer and PBT possible. © 2000 John Wiley & Sons, Inc. J Appl Polym Sci 75: 361–370, 2000

Key words: PP-PBT blends; PP-PPE blends; Polypropylene compatibilizers; Polypropylene-Phenol formaldehyde copolymers; Reactive extrusion

INTRODUCTION

In the first part of this series (I), the synthesis of polypropylene-*graft*-phenol formaldehyde copolymers was demonstrated.[1] For this synthesis, it was clearly shown that the component viscosity ratio had a significant effect on the conversions of the reactants. Component viscosity ratios of close to 1 were observed to give optimum reaction conversions. This is also according to earlier stated theories.[2,3] In the second part (II), the application of polypropylene-*graft*-phenol formaldehyde copolymers as compatibilizers for polypropylene/polyamide (PP/PA6) (75/25) blends were evaluated.[4]

The present study was aimed at understanding the relationship between the nature of the compatibilizer and the resulting blend properties. In particular, PP/poly(butylene terephthalate) (PBT) and PP/PPE blends with were investigated.

EXPERIMENTAL

Materials

Three isotactic PP–polyethylene (PE) heterophase block copolymers, one PBT, and one poly(phenylene ether) (PPE) grade provided the poly-

Correspondence to: K. L. Børve, Borealis AS, Department of Polymer Development, Rønningen, N-3960 Stathelle, Norway.

Contract grant sponsors: Norwegian Research Council (NFR); Borealis AS, Bamble.

Journal of Applied Polymer Science, Vol. 75, 361–370 (2000)
 CCC 0021-8995/00/030361-10

Table I Blend Formulations from Experimental Design

Trial No.	PBT/PPE Content (wt %)	η_{PBT}/η_{PP}[a] η_{PPE}/η_{PP}	PP-*g*-PF (wt %)	Extruder (rpm)
1	17.5	2	3	100
2	10	3	1	175
3	10	1	1	250
4	25	3	5	175
5	17.5	3	1	250
6	10	3	5	100
7	10	3	5	250
8	25	3	5	250
9	25	1	5	100
10	10	1	1	100
11	10	1	5	175
12	25	3	1	100
13	10	3	3	250
14	10	3	5	100
15	10	1	3	175
16	17.5	1	1	175
17	25	1	1	175
18	25	1	5	250
19	10	2	1	175
20	25	1	5	100
21	25	3	1	100
22	25	3	1	250
23	10	1	1	250
24	10	2	5	250
25	10	1	1	100

[a] Viscosity measured at 500 s^{-1}.

mers. PP P 350FB, P 330FB, and P410H were supplied by Borealis. The measured MFI of these PPs were 12, 5.5, and 0.9 g/10 min (230°C/2.16 kg), respectively. PBT Vestodur VD 2000 (MFI 14 mL/10 min (250°C/2.16 kg)) and PPE Vestoran X4893 (density 1.06 g/cm^3) were both supplied by Hüls. Compatibilizers based on PP–phenol formaldehyde (PF) were synthesized according to an in-house procedure (PP-*g*-PF).[1–4] This PP-*g*-PF compatibilizer was characterized by 45% PF by weight and had a PF molecular weight, M_n, of 27,550 g/mol.

Experimental response surface modeling was used to generate the blend formulations used in the first part of this study. Designing was done using Modde 3.0 software from Umetri AB in Sweden. The 25 trials' design based on an quadratic model with five replicates are presented in Table I. Two equal designs were run, one for each of the engineering polymers, PBT and PPE.

In addition, blends of PP/PBT were prepared with 0.15, 0.22, 0.31, 0.4, 0.48, 0.56, 0.63, 0.70, and 0.8 volume fractions of PF. Blends without and with a 5 wt % compatibilizer were prepared.

For the design trials and the concentration curves, the amount of base polymer (PP) in the blend was decreased according to the compatibilizer concentration. The PP-*g*-PF compatibilizer and the PBT and PPE were predried at 80°C for 12 h to remove residual monomers and traces of water.

Blending

The preparation of the PP–PF graft copolymers was conducted in a 25-mm Clextral BC 21 intermeshing corotating twin-screw extruder (TSE) with an *L/D* of 44. PP, the compatibilizer, and PBT/PPE were all fed into barrel 3 at a total throughput of 3 kg/h. The screw rotation speed was 150 rpm and the barrel set temperature 250–270°C for the PBT blends and 255–285°C for the PPE blends. Average residence time at these conditions was 2.5 min. The extruder was equipped with highly efficient vacuum venting to remove unreacted species and reaction by-products. An inert atmosphere was used to reduce polymer degradation. The extrudate was immediately quenched in a water bath and then pelletized.

The extruder screw profile was configured to allow good melting of the polymers followed by efficient mixing and high shear, high residence time in the reaction zone, and venting at the outlet of the extruder. Neutral, 90°, kneading blocks followed by backmixing screw elements were located after 10 *L/D* and 25 *L/D*. The remaining elements of the screw profile were semipitch conveying elements. The extruder was equipped with a K'tron loss-in-weight feeding system for accurate feeding of the raw materials.

Sample Preparation and Characterization

A systematic chemical and mechanical characterization of the blends was undertaken using rheologic, microscopic, and mechanical testing. Melt viscosity was analyzed using a Bohlin CSM rheometer equipped with 25-mm parallel plates and 1-mm gap setting. The rheometer was modified to reduce polymer degradation during analysis.

Blend morphology was investigated with a scanning electron microscope (SEM, JEOL T 300). The micrographs were taken of extrudates collected from the TSE. The samples for SEM

were prepared by fracturing at liquid nitrogen temperature and they were gold-plated before microscopy. Average particle was determined using image analysis techniques.

Test samples for tensile and some of the impact testing samples were injection-molded on an Arburg 150-45 all round 170 CMD injection-molding machine. Molding temperature was 250–270°C for PBT and 260–275°C for PPE, and all samples were molded at the same conditions. The samples were dried at 80°C for 12 h prior to injection molding. Tensile specimens of a dogbone type and an impact testing disc of 2 mm were molded.

Tensile testing was performed with a Zwick tensile tester 1445 according to ISO R 527. The test temperature was 23°C. Impact testing was conducted on a Rosand instrumented falling weight impact tester, type 5, according to ISO 6603/1. Samples were tested at 0°C. The injection-molded samples were dried at 80°C for 12 h prior to testing and stored in sealed bags until testing.

Analysis of the designs were done using Modde 3.0 software. The analysis was based on PLS techniques.[5,6]

RESULTS AND DISCUSSION

Viscosities of Component Polymers

The melt viscosity ratios as a function of shear rate for PBT and PP and PPE and PP are shown in Figures 1 and 2, respectively. Since the measuring temperature was almost the same as the extrusion temperature, about 250°C, the measured viscosity ratios indicate the ratio that dominated under the processing conditions. Typical shear rates during reactive extrusion will be 10^2–10^3 s^{-1}.[7] During extrusion at normal conditions, viscosity ratios of about 1, 2, and 3 were obtained, depending on the PP grade.

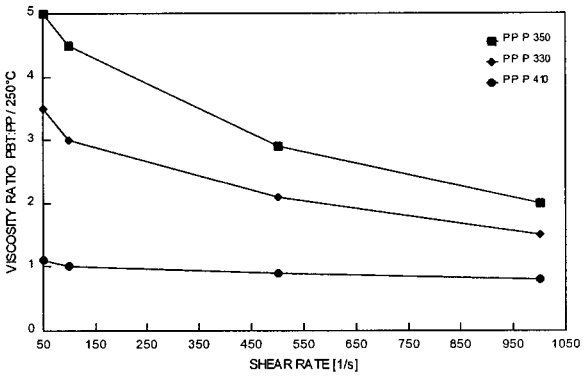

Figure 1 Complex viscosity ratio versus shear rate (s^{-1}) at 250°C for PP/PBT.

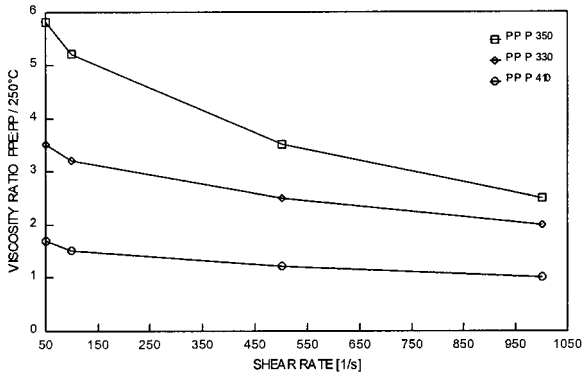

Figure 2 Complex viscosity ratio versus shear rate (s^{-1}) at 250°C for PP/PPE.

Response Modeling of PP/PBT Blends

Response modeling of the PP/PBT design and corresponding response values collected from mechanical testing was done using PLS techniques in the Modde 3.0 software. These results are presented as 2-D contour plots where two variables are plotted on each axis, and the response values are shown at the contour lines. The two remaining variables were fixed at a specified level for each plot. It should also be emphasized that any maximum or minimum levels that have been presented here are related to the experimental frame of this study. Other minima or maxima may exist outside this frame.

When generating the experimental design for the PP/PBT blends, 10–25 wt % contents of PBT were used. In this PBT concentration range, no phase inversion from PP to PBT as the continuous phase was expected. This is an important consideration when making such designs, to avoid the discontinuity which a phase inversion represents, and, therefrom, the danger of making wrong conclusions.

The mechanical properties of the starting PP polymers were not very different. The elastic moduli ranged from 1050 to 1300, P 410H being the lowest, and P330FB, the highest. The impact strength varied more; P 410H was measured to 18 J, and P 350FB, to 7 J. In the figures where the viscosity ratio is given on one of the variable axes, some variations from the original properties of the polymers also confounded the results. The

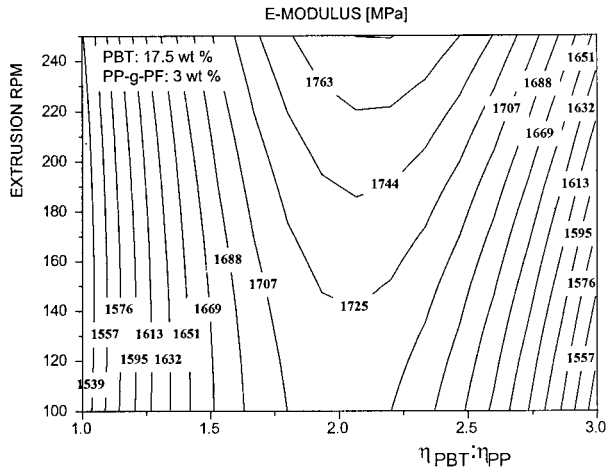

Figure 3 2-D contour plot of E modulus versus PBT/PP viscosity ratio and extruder rpm. PP-*g*-PF: 3 wt %; PBT: 17.5 wt %.

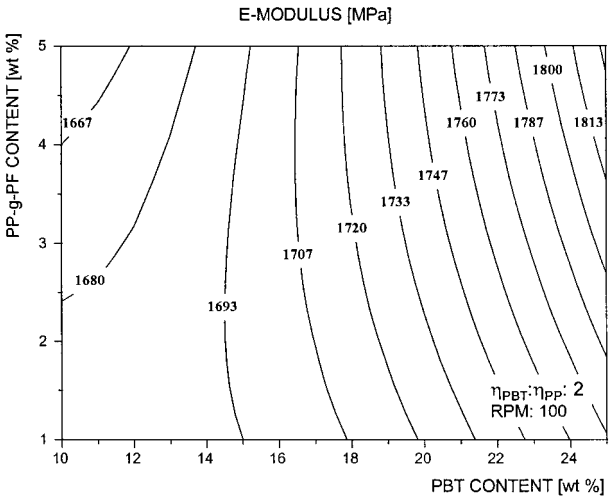

Figure 4 2-D contour plot of E modulus versus PBT content and PP-*g*-PF. Rpm: 100; PBT/PP viscosity ratio: 2.

absolute effect on the responses from the viscosity ratio only will not be presented. However, the trends have been checked by similar curves with the relative properties calculated from the rule of mixture. These trends correspond to the trends for the absolute values.

The relationships among the viscosity ratio (500 s^{-1}), extrusion rpm, and elasticity modulus is presented in Figure 3. The figure clearly shows that maximum E modulus was obtained at a viscosity ratio (PBT/PP) at about 2 and with 250 rpm. PBT and PP-*g*-PF contents were fixed at 17.5 and 3 wt %, respectively. An E modulus of 1700 MPa was observed.

In Figure 4, the E modulus is presented as a function of PBT content and PP-*g*-PF compatibilizer content. At a fixed PBT/PP viscosity ratio of 2 and extrusion rpm of 100, the highest E modulus (1820 MPa) was achieved at 25 wt % PBT and 5 wt % PP-*g*-PF. The slope of the contour curves also indicated that the E modulus was less dependent on PP-*g*-PF than on PBT, especially at higher PBT contents. The minimum E modulus was found at 10 wt % PBT and 5 wt % PP-*g*-PF.

A similar plot is given in Figure 5, the only difference being the rpm of 250. This figure also shows that the highest E modulus was obtained at 25 wt % PBT and 5 wt % PP-*g*-PF: An E modulus of 1915 MPa was obtained. In this case, the elastic modulus was more dependent on the PP-*g*-PF content than for 100 rpm. The lowest E modulus was observed at the lowest PBT and PP-*g*-PF content.

Impact strength as a function of the PBT/PP viscosity ratio and extrusion rpm is given as a 2-D contour plot in Figure 6. The overall picture was different from the E modulus, and the maximum level of impact was reached at a viscosity ratio of 1 and extrusion rpm of about 200. This result also confirms the general weakness of the blending of immiscible polymers, where there is a lack of sufficient dispersivity and interphase adhesion. The role of blend composition and compatibilization will therefore be essential for the final mechanical properties and, especially, for the impact strength. Impact is plotted as a function of PBT and PP-*g*-PF content for a PBT/PP viscosity ratio

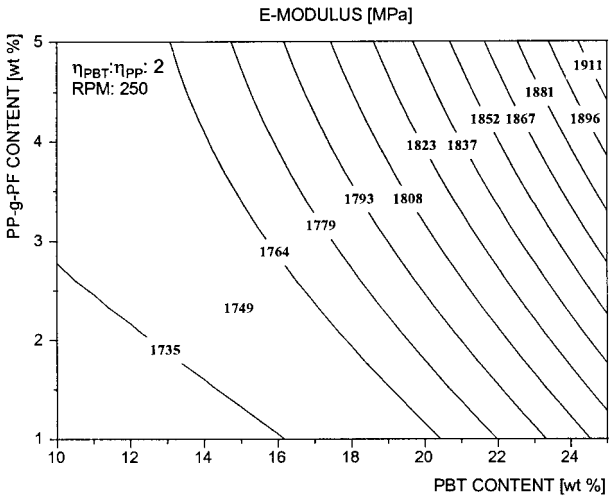

Figure 5 2-D contour plot of E modulus versus PBT content and PP-*g*-PF. Rpm: 250; PBT/PP viscosity ratio: 2.

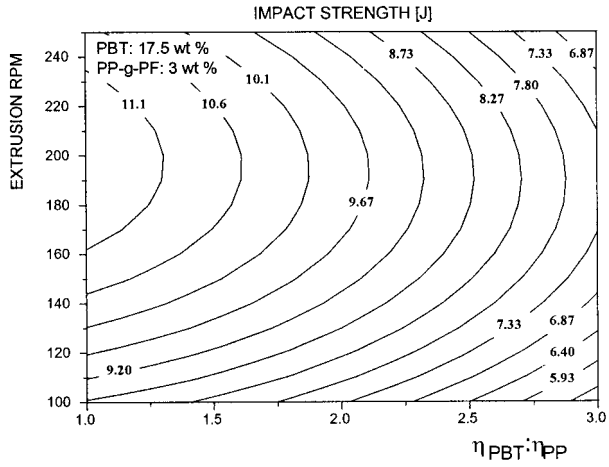

Figure 6 2-D contour plot of impact strength versus PBT/PP viscosity ratio and extruder rpm. PP-*g*-PF: 3 wt %; PBT: 17.5 wt %.

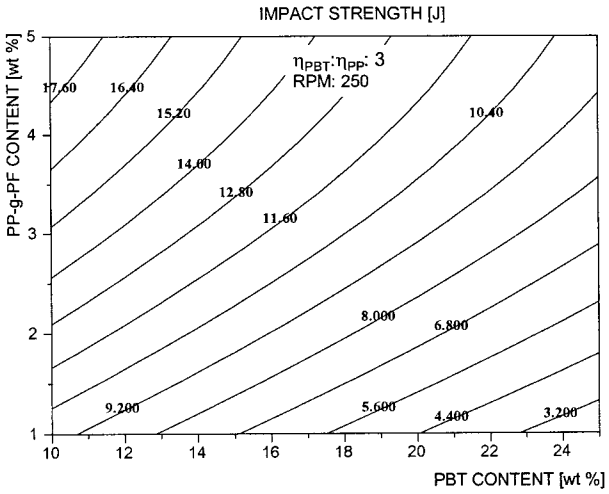

Figure 8 2-D contour plot of impact strength versus PBT content and PP-*g*-PF. Rpm: 250; PBT/PP viscosity ratio: 3.

of 1 and 100 rpm (Fig. 7), and 250 rpm (Fig. 8). In both figures, the highest impact strengths were obtained at low PBT (10 wt %) and high compatibilizer content (5 wt %). The highest impact values were found in the case of 250 rpm. The reason for this is probably that the additional dispersion achieved by high-energy mixing combined with a high content of the compatibilizer will reduce the average particle size of the dispersed phase and thereby increase the impact strength.

Response Modeling of PP/PPE Blends

Similarly, the response modeling of the PP/PPE design and corresponding response values collected from mechanical testing was done using PLS techniques in the Modde 3.0 software.

The relationships among the PPE/PP viscosity ratio at 500 s^{-1}, extrusion rpm, and elasticity modulus is presented in Figure 9. This 2-D figure clearly shows that the maximum *E* modulus was obtained at a viscosity ratio (PPE/PP) of about 2 and at 250 rpm. This is similar to the best conditions observed for PBT. PPE and PP-*g*-PF contents were fixed at 17.5 and 3 wt %, respectively. At these settings, an *E* modulus of 1690 MPa was observed.

A 2-D contour plot of the *E* modulus as a function of PPE content and PP-*g*-PF compatibilizer

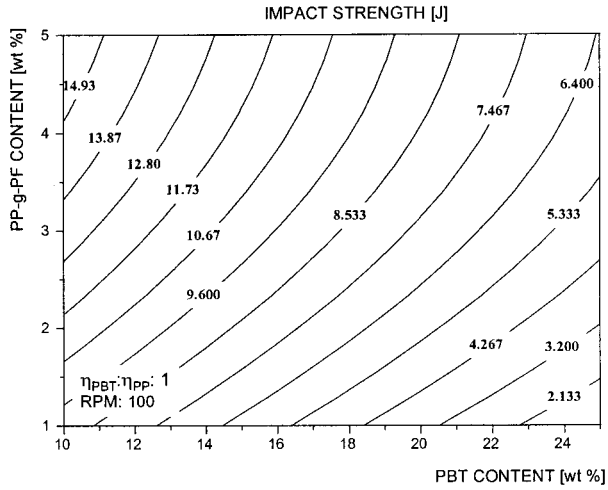

Figure 7 2-D contour plot of impact strength versus PBT content and PP-*g*-PF. Rpm: 100; PBT/PP viscosity ratio: 1.

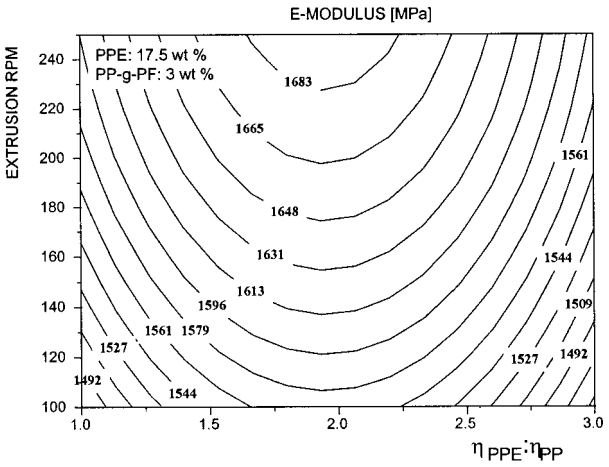

Figure 9 2-D contour plot of *E* modulus versus PPE/PP viscosity ratio and extruder rpm. PP-*g*-PF: 3 wt %; PPE: 17.5 wt %.

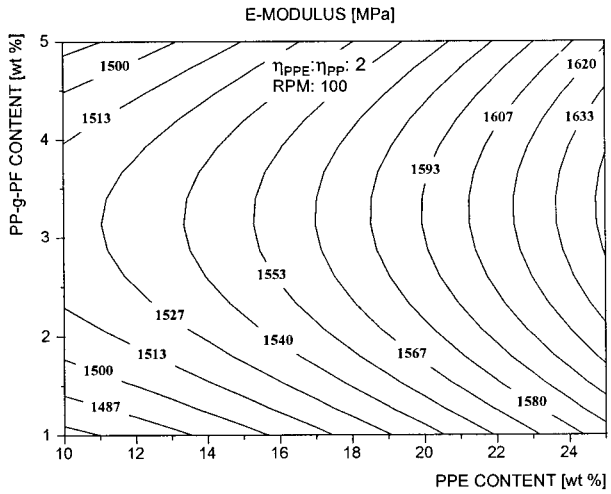

Figure 10 2-D contour plot of *E* modulus versus PPE content and PP-*g*-PF. Rpm: 100; PPE/PP viscosity ratio: 2.

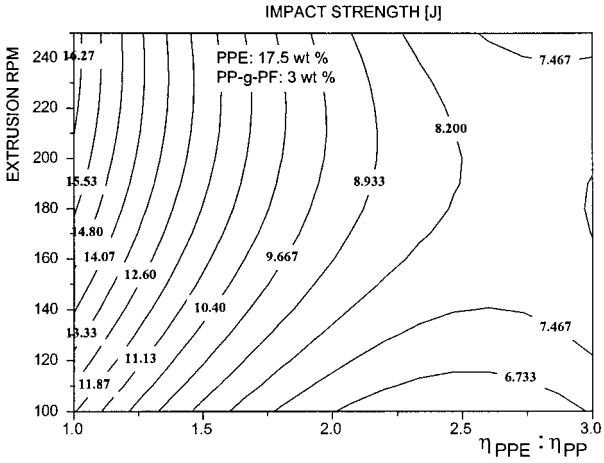

Figure 12 2-D contour plot of impact strength versus PPE/PP viscosity ratio and extruder rpm. PP-*g*-PF: 3 wt %; PPE: 17.5 wt %.

content is presented in Figure 10. A PPE/PP viscosity ratio of 2 and extrusion rpm of 100 were kept constantly. The highest *E* modulus of 1650 MPa was achieved at 25 wt % PBT and 3.1 wt % PP-*g*-PF. The minimum *E* modulus was found at 10 wt % PPE and 3.1 wt % compatibilizer. A similar 2-D plot for 250 rpm is shown in Figure 11. At these conditions, the maximum *E* modulus was achieved at 25 wt % PPE and 5 wt % compatibilizer. A higher maximum elastic modulus was also observed at 1850 MPa.

A 2-D contour plot of the impact strength as a function of the PPE/PP viscosity ratio and extrusion rpm is presented in Figure 12. Again, the observed viscosity ratio dependency was different from the case of the elastic modulus. Maximum impact was reached at a viscosity ratio of 1 and extrusion rpm of about 250. However, a minimum impact strength, a probable local minimum, was obtained at the viscosity ratio 2.75 and about 200 rpm. Figures 13 and 14 show 2-D contour plots of the impact strength as a function of PPE and PP-*g*-PF content for a PPE/PP viscosity ratio of 1 and 100 rpm (Fig. 13) and 250 rpm (Fig. 14). In both figures, the highest impact strengths were obtained at low PBT (12 wt %) and high compatibilizer content (5 wt %). Impact strength values of

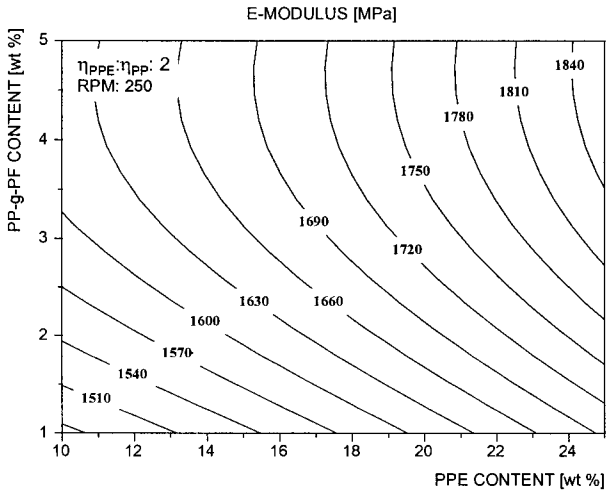

Figure 11 2-D contour plot of *E* modulus versus PPE content and PP-*g*-PF. Rpm: 250; PPE/PP viscosity ratio: 2.

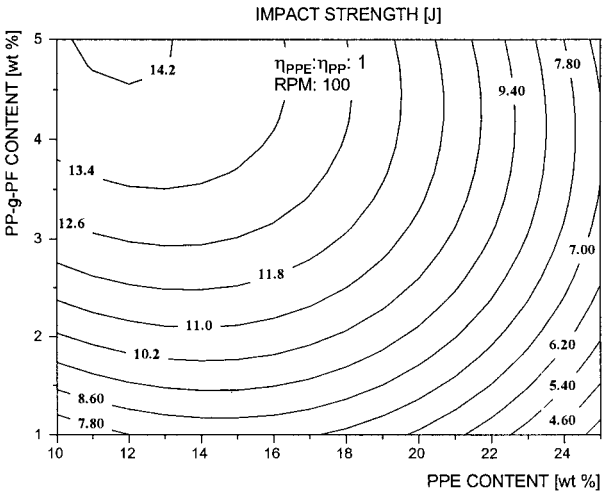

Figure 13 2-D contour plot of impact strength versus PPE content and PP-*g*-PF. Rpm: 100; PPE/PP viscosity ratio: 1.

14.5 and 20.5 J were achieved for 100 and 250 rpm, respectively. The poorest impact strength was observed for blends of high PPE content (25 wt %) and low compatibilizer content (1 wt %). In this case, also, the minimum impact strength was generally higher for extrusion at 250 rpm than at 100 rpm. The main explanation for this is probably that the additional dispersion achieved by high-energy mixing, combined with high content of the compatibilizer, will reduce the average particle size of the dispersed phase and thereby increase the impact strength. At high PPE and low compatibilizer loadings, too low a concentration of PP-*g*-PF is present at the PPE/PP interface, giving poor interface stabilization and adhesion. This again will result in poor impact strength.

Phase Inversion of PP/PBT Blends

For the determination of morphology development with increasing content of PBT, six blends with 0.15–0.8 volume fractions of PBT, and without the compatibilizer, were prepared. In addition, six blends with 5 wt % compatibilizer were prepared to determine the effect of the PP-*g*-PF compatibilizer on the blend morphology. The blends were all prepared in the TSE at the same conditions. The morphology of the noncompatibilized blends of PP/PBT was so coarse that the phase inversion could be determined by using an optical microscopy and hot stage. The melting of the individual phases was observed, to determine whether the melting first took place in the dispersed or the continuous phase.

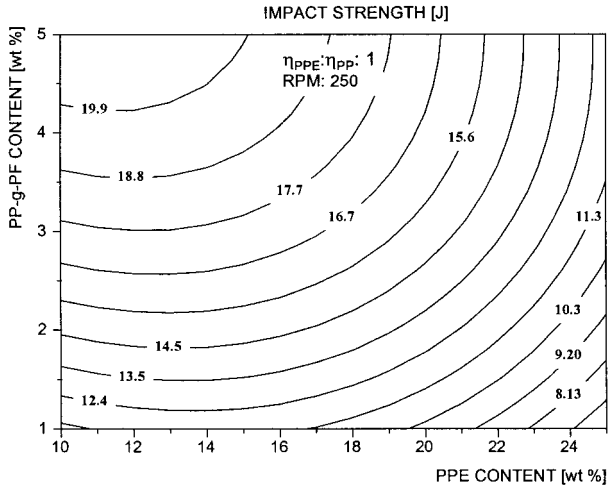

Figure 14 2-D contour plot of impact strength versus PPE content and PP-*g*-PF. Rpm: 250; PPE/PP viscosity ratio: 1.

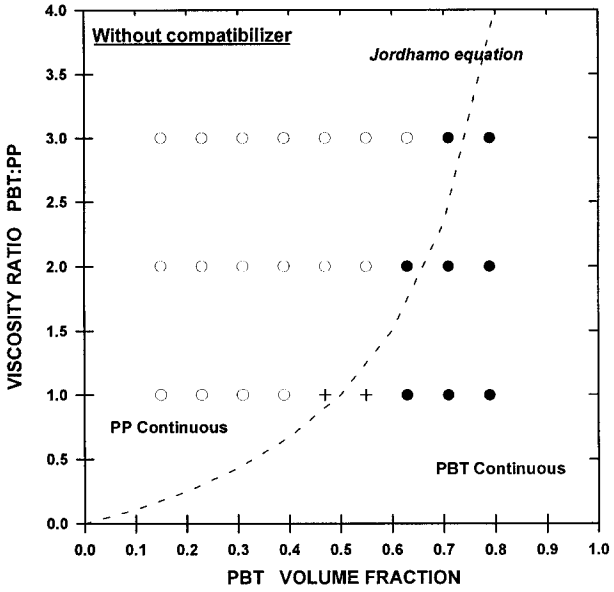

Figure 15 Phase-inversion regions of the PP/PBT blend containing no compatibilizer.

Jordhamo et al.[8] developed an empirical model for the prediction of the phase-inversion behavior of immiscible polymer blends. This model is based on prediction of the phase-inversion regions as a function the melt viscosity and volume fractions. According to the model, phase inversion occurs when the following equation is valid:

$$\frac{\eta_m \times \theta_d}{\eta_d \times \theta_m} = 1$$

where η is the viscosity and θ is the volume fraction. m and d are the matrix and the dispersed phase, respectively. Jordhamo's equation is generally limited to low shear rates.

The phase-inversion behavior of the noncompatibilized blends is depicted in Figure 15. The viscosity ratio was determined from the rheology measurements (Fig. 1) at an estimated average shear rate of 500 s^{-1}. This shear rate was earlier reported to be a typical average shear rate for reactive extrusion processing. The figure shows that the lower the viscosity ratio, the lower was the PBT concentration at which phase inversion was observed. Jordhamo's model for phase behavior is added to the figure. The model correlates fairly well with the experimental results, also indicating that the model is valid for the shear rate at 500 s^{-1}, which was estimated to be the average shear rate of the extruder.

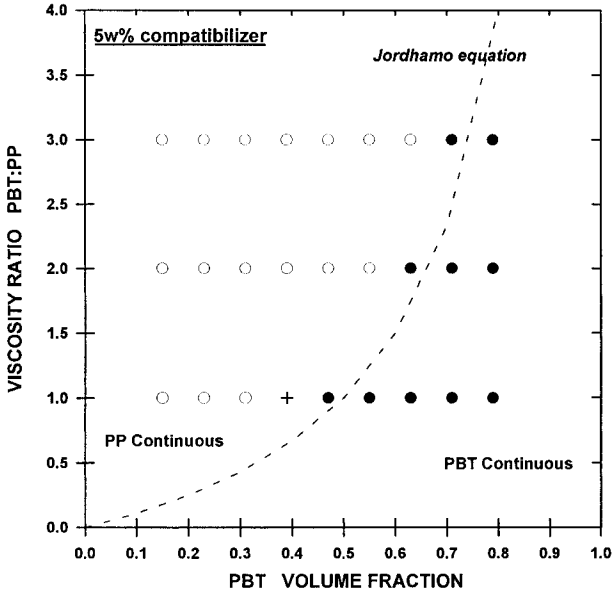

Figure 16 Phase-inversion regions of the PP/PBT blend containing 5 wt % compatibilizer.

PP-*g*-PF was reported earlier to be an efficient compatibilizer for PP/PA6 blends based on morphology studies and mechanical performance of the blends. Similar improvements of the PP-*g*-PF compatibilizer in PP-based blends with 10–30 wt % PBT were indicated earlier in this present article. The morphology of the compatibilized blends is below the resolution threshold of optical microscopy, and SEM was used. The phase-inversion behavior of the compatibilized blends is depicted in Figure 16. The viscosity ratios were similarly determined from the rheology measurements (Fig. 1) at a shear rate of 500 s^{-1}. Compared to the noncompatibilized blends presented in Figure 15, addition of the compatibilizer changed the range of phase inversion only for the P 410H/PBT having a viscosity ratio of about 1. For these blends, dual-phase continuity was observed at a PBT concentration of 40% by volume or 0.49 wt %. It was also evident that the PP-*g*-PF compatibilizer did not have a pronounced effect on composition of the phase inversion. The same conclusion was also reported for PP/PA 66 systems.[9]

Blend Morphology

The addition of the compatibilizer changed the morphology of the blends considerably. The noncompatibilized blends of PP with 30 wt % PBT had a coarse morphology with average domain sizes as large as tens of microns (Fig. 17). This large particle size confirms the incompatibility of the two polymers. The blend morphology of the compatibilized PP-based blends with 30 wt % PBT and 5 wt % PP-*g*-PF is shown in Figure 18. In the compatibilized blend, the morphology was much finer, with the average particle size of about 1 micron.

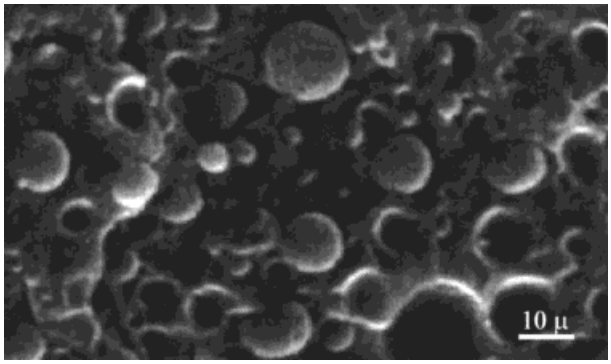

Figure 17 SEM picture of incompatibilized PP/PBT blend.

A noncompatibilized blend of 30% PPE and PP resulted in the same coarse morphology as for the noncompatibilized PP/PBT blends. The blend morphology of the compatibilized PP-based blends with 30 wt % PPE and 5 wt % PP-*g*-PF is shown in Figure 19. In the compatibilized blend, the morphology was much finer, with an average particle size of some 4–5 microns. However, the same interphase adhesion is not observed in this case as for the PP/PBT blend. The reason for this is probably that this PPE grade was end-capped; no reaction with any free end-groups was possible. The stabilization effect of the PP-*g*-PF is more or less due

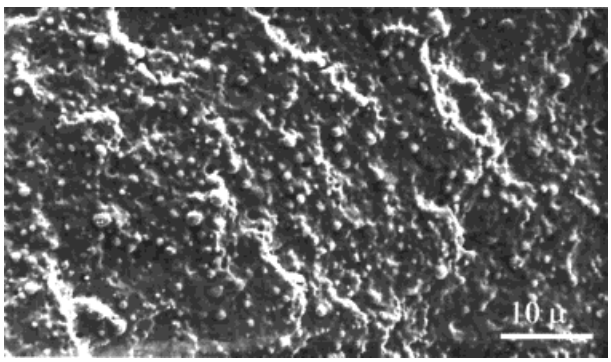

Figure 18 SEM picture of compatibilized PP/PBT blend.

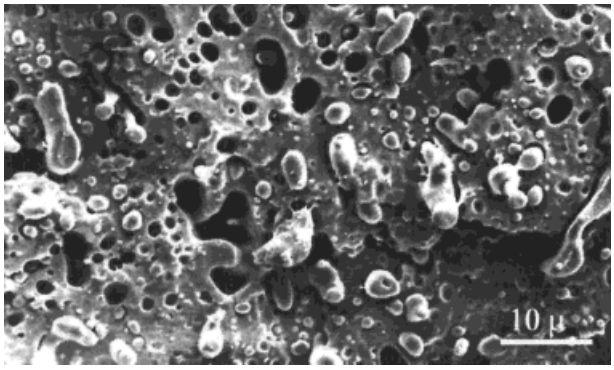

Figure 19 SEM picture of compatibilized PP/PPE blend.

to π–π orbital overlap, giving relatively strong secondary attraction.

In the case of PBT, the PBT grade was analyzed by titration to contain about 40 mmol/kg of —COOH and 15 mmol/kg of —OH, as available end-groups. The carboxylic end-groups will have a potential of reacting with the primary —OH end-groups of the PF part of the compatibilizer. This reaction was checked by studying a model system of PBT and PF, 75/25 (wt/wt). This blend was extruded at the same conditions as used for the PP/PBT blending, and samples were quenched, extracted for any unreacted PF, and then analyzed by FTIR. When comparing the FTIR spectrum with the corresponding spectrum of PF and PBT (Fig. 20), there was a change in the aromatic ring stretch at 1593 cm^{-1}, indicating that a reaction between PBT and PF had occurred. No effort was done to quantify this reaction. In addition, the same stabilization effect of the PP-*g*-PF from the π–π orbital overlap is expected also for the PBT blends.

CONCLUSIONS

Compatibilizers based on PP and PF (PP-*g*-PF) were suitable for blends or alloys of PP and engineering polymers having aromatic residues or functionality complimentary to hydroxyl. Blends of isotactic PP and PBT and PPE were well compatibilized by PP-*g*-PF. The phase-inversion behavior followed the Jordhamo's model,[8] and this could be used to predict the continuous phase.

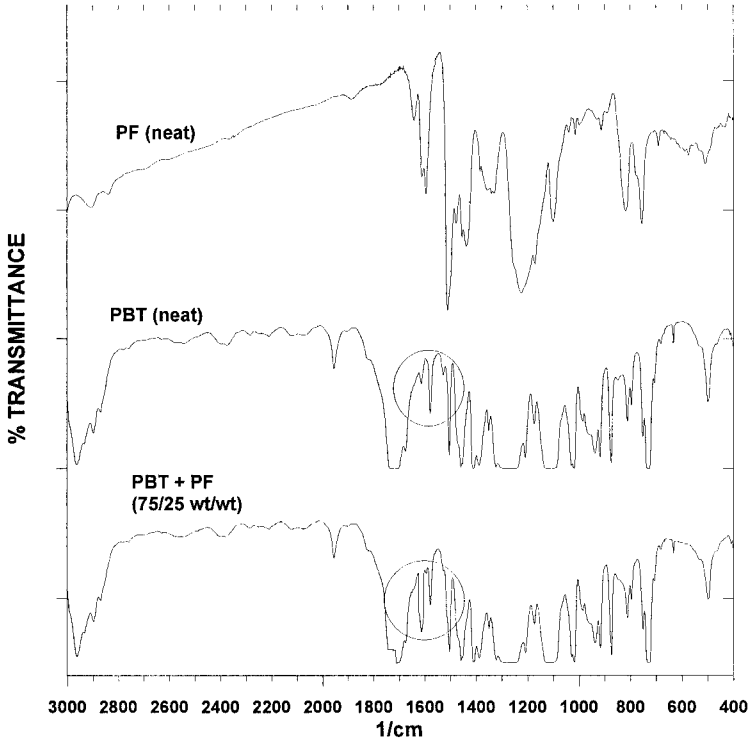

Figure 20 FTIR spectrum of neat PF, neat PBT, and a reactive blend of PBT/PF (75/25).

The PP-*g*-PF compatibilizer was observed to be more efficient in blends of PBT than of PPE.

NOMENCLATURE

PP	polypropylene
PF	phenol formaldehyde resin
PBT	poly(butylene terephthalate)
PPE	poly(phenylene ether)
MAH	maleic anhydride
PP-*g*-MAH	MAH-grafted PP
PP-*g*-GMA	GMA-grafted PPT
PP-*g*-PF	PP-*graft*-PF compatibilizer

This work was part of a Ph.D. thesis and could not have been performed without the help of a number of people at Borealis AS and The Norwegian Institute of Science and Technology, Department of Machine Design and Materials Technology. This work was financed by the Norwegian Research Council (NFR) and Borealis AS, Bamble.

REFERENCES

1. Børve, K. L.; Kotlar, H. K.; Gustafson, C.-G. submitted for publication to J Appl Polym Sci.
2. Rauwendaal, C. Polymer Extrusion; Hanser: Munich, 1985.
3. Rauwendaal, C. Mixing in Polymer Processing; Marcel Dekker: New York, 1991.
4. Børve, K. L.; Kotlar, H. K.; Gustafson, C.-G. submitted for publication to J Appl Polym Sci.
5. Atkinson, A. C.; Donev, A. N. Optimum Experimental Designs; Oxford University: New York, 1992.
6. Krzanowski, W. J. Principles of Multivariate Analysis: A User's Perspective; Oxford University: New York, 1992.
7. Eisele, U. Introduction to Polymer Physics; Springer-Verlag: New York, 1990.
8. Jordhamo, G. M.; Manson, J. A.; Sperling, L. H. Polym Eng Sci 1986, 26, 517.
9. Hietaoja, P. T.; Holsti-Miettinen, R. M.; Sepälä, J. V.; Ikkala, O. T. J Appl Polym Sci 1994, 54, 1613.